Open Access

Polarization Coupling Based on Faraday Effect in Whispering-Gallery-Mode Resonator

Yijie Nie
Mengfan Xu
Xin Zhang
Mi Li
Yuejiang Song

1st supermode
2nd supermode

Polarization Coupling Based on Faraday Effect in Whispering-Gallery-Mode Resonator

Yijie Nie [ID], Mengfan Xu, Xin Zhang, Mi Li [ID], and Yuejiang Song [ID]

Key Laboratory of Intelligent Optical Sensing and Manipulation, College of Engineering and Applied Science, Nanjing University, Nanjing 210093, China

Abstract: In this article, we study the polarization coupling in a Faraday magnetooptical microcavity. Due to Faraday effect, the polarization coupling can be achieved between the intrinsic left and right elliptically-polarized modes. The mode characteristics of the Faraday microcavity, such as the dispersion curve, mode distribution and polarization evolution, are studied. And the supermodes can generate the different elliptical polarization with the different ellipticity and orientation angles. This polarization coupling may have potential applications related to polarization modulation.

Index Terms: Faraday effects, whispering-gallery mode (WGM), polarization coupling.

1. Introduction

Whispering-Gallery mode (WGM) resonators with high Q factor and small mode volume have been got intensive applications in modern photonics [1], including ultra-low-threshold narrow-linewidth lasers [2], [3], ultra-sensitive bio-sensing [4], [5] and frequency combs [6], [7]. Faraday effect has been long discovered and played an important role in physics, such as quantum optics and spintronics. In 1845, Michael Faraday discovered a beam of plane-polarized light was rotated as it passed through a medium in a uniform magnetic field [8]. This effect indicated the interaction between the magnetic field and the light. Based on this effect, many magneto-optic (MO) devices such as MO magnetic field sensors [9], MO modulators [10], and isolators [11], [12] have been invented. Recently MO microcavities have been researched widely because it can provide a platform of enhanced MO interaction. For example, in the yttrium iron garnet (YIG) sphere, strong coupling between microwave photons and magnons has been observed [13]. Also, Brillouin scattering is greatly enhanced through triply resonant magnon, signal light, and pump light in YIG microspheres [14], [15]. And the nonreciprocity and asymmetry in the sideband signals generated by the magnon-induced Brillouin scattering of light are observed [16]. What's more, the researcher demonstrated that magneto-optical coupling could be generated by the combined Voigt effect and Faraday effect [17]. The static direction of the magnetization tuned the resonant frequency through the Voigt effect and the degree of polarization rotation through the Faraday effect. The nonreciprocity was demonstrated through the spin-orbit coupling in the high Q ferromagnetic microspheres [18]. But until now, the polarization coupling has not been studied in the MO microcavity although it can play a very important role in the resonant MO microcavity.
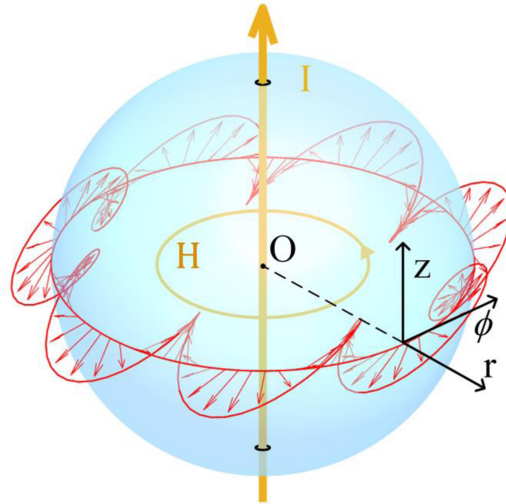
Fig. 1. The proposed Faraday microcavity. The direction of axisymmetric magnetic field H, generated by the current I through the sphere center, is parallel to the propagation direction ϕ of the resonant elliptically- polarized mode.

In this paper, we will theoretically study the mode characteristics in the MO microcavity that is only affected by the Faraday effect. In this Faraday microcavity, the polarization coupling between the intrinsic elliptically polarized modes can be generated due to Faraday effect. Compared with the regular elliptical polarization of the intrinsic mode, the supermode exhibits the oblique elliptical polarization with different orientation and ellipticity angles due to the polarization coupling. This polarization coupling may be of interest in applications related to polarization modulation.

2. Proposed Faraday Magnetooptical Microcavity

The proposed MO cavity in the cylindrical coordinate system (r, ϕ, z) is shown in Fig. 1. The resonator is a dielectric microsphere imposed by an axisymmetric magnetic field H. Such the field can be generated by the current flowing through a small tunnel that passes through the sphere diameter along the axial direction (z) of cylindrical coordinates, as shown in Fig. 1. The WGMs in this microsphere are supposed to not be affected by the existence of such a tiny tunnel. The dielectric material can be any material, such as ferromagnetic material, optical glass and so on. In this paper we choose the fused silica as our material for the theoretical research without losing any generality. But in terms of the experiment, ferromagnetic material is a better choice due to their intrinsic magnetization. The radius R of the microsphere cavity is fixed at 100 μm and the resonant wavelength is in the 1550 nm waveband.

The direction of axisymmetric magnetic field H generated by the current I is parallel to propagation direction of the resonant WGM in the microcavity, therefor the resonator mode is only affected by the Faraday effect. We name such the microcavity which is only affected by the Faraday effect as a Faraday microcavity.

Within the macroscopical theory of magnetoptical phenomena, the properties of a medium are defined by the permittivity tensor ε and permeability tensor μ. Due to the presence of a magnetic field, the permittivity tensor ε of the material has changed [19], [20]. In our silica Faraday microcavity, with magnetic field H along the ϕ direction, the ε tensor becomes a sum of asymmetric and symmetric tensors in cylindrical coordinates:

$$\varepsilon = \begin{bmatrix} \varepsilon_1 & 0 & 0 \\ 0 & \varepsilon_1 & 0 \\ 0 & 0 & \varepsilon_1 \end{bmatrix} + \begin{bmatrix} 0 & 0 & -ig \\ 0 & 0 & 0 \\ ig & 0 & 0 \end{bmatrix} \tag{1}$$
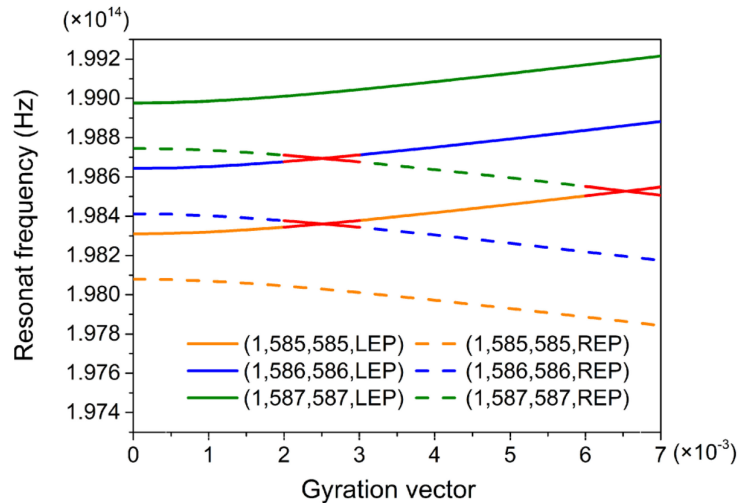
Fig. 2. Resonant frequency of different mode in Faraday microsphere.

where ε_1 is the permittivity of silica, and $\varepsilon_1 = 1.4440^2$ in the 1550 nm waveband at room temperature [21]. g is the gyration vector, and its vector direction is only related to the direction of the magnetic field H and its magnitude is proportional to the intensity of H as well as Verdet constant V [20]. In our structure, the direction of gyration vector g is the axisymmetric ϕ direction and its magnitude can be changed by the current I. In the following study, we will neglect absorption losses of the material and focus on the results from g. The gyration vector g is also seen as a scalar quantity of its magnitude.

3. Results and Discussions

In this paper, we use the Finite-element method (COMSOL Multiphysics 5.2a) to calculate the mode properties in an axisymmetric Faraday dielectric resonator [22]. Firstly, according to the ε tensor of Equ. (1), the weak-form solutions to Maxwell's equations are derived for the Faraday microcavity. Then PDE (partial-differential-equation) solver of COMSOL is used to solve these weak forms to achieve the mode properties at different g, including the frequency, field distribution, Q factor and polarization of the resonant mode. In the whole calculations, we find that the ϕ-component of optical field H can be omitted because it is far smaller than two other components in the directions r and z.

When the light propagates along the circumstance of the microsphere cavity, the optical mode is totally reflected at the dielectric-air boundary and forms WGM. The WGM of a dielectric sphere microcavity can be characterized by a set of four quantum numbers (n, l, m, p), where n denotes the radial mode number, l the angular mode number, m the azimuthal mode number as well as p the polarization. Each azimuthal mode number m ranges from $l \ldots -l$. In an ideal silica microsphere without any MO effect, each resonant frequency will have a $(2l + 1)$ degeneracy with respect to the azimuthal mode number m. And the typical polarizations of WGMs are the linear polarizations, i.e., the transverse electric (TE) polarization or the transverse magnetic (TM) polarization.

But in a Faraday microcavity, the WGMs must be affected by the gyration vector g additionally. In order to understand the modal characteristics of the WGMs in Faraday microcavity, we investigate the modal dispersion relations of some fundamental modes ($n = 1$, $m = l$) with the gyration vector g. The intrinsic mode is the resonant mode in Faraday microcavity when there is no coupling between the different modes. Fig. 2 shows the dependences of the resonant frequencies of three pairs of intrinsic resonant modes on the gyration vector g. A pair of the resonant modes is defined as two resonant modes possessing the same (n, l, m) but two orthogonally elliptical polarizations. All these modes have the similar Q factor of the order of 10^7 and almost don't change with g.
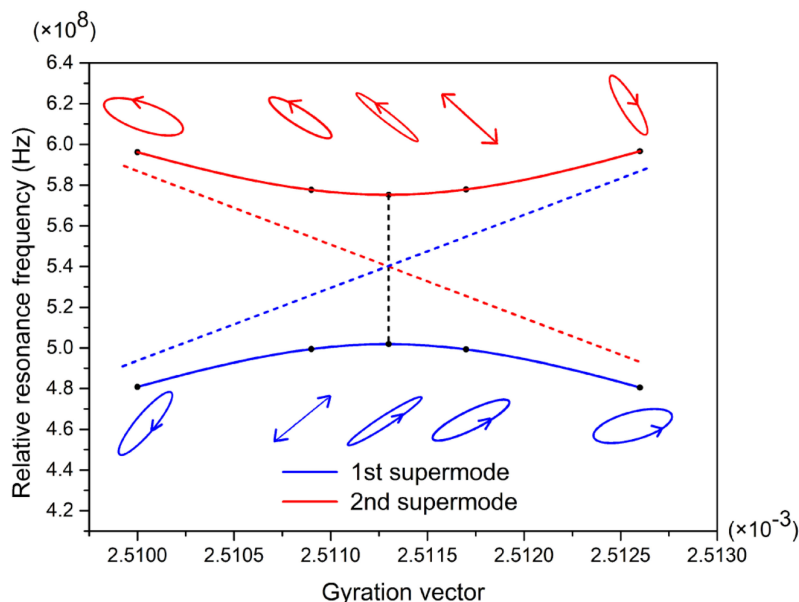
Fig. 3. The dispersion curves and polarizations of mode coupling between the mode (1, 586, 586, LEP) and the mode (1, 587, 586, REP).

As we have known, for each pair of modes, when $g = 0$ (without the Faraday effect), these two modes are the TE- and TM-polarized modes, which is shown in Fig. 5 where $g0 = 0$. Their resonant frequencies are different from each other due to their intrinsic mode birefringence index. And the frequency of TM mode is larger than that of TE mode. In our structure of silica sphere with 100 um radius, the permittivity difference between two modes is calculated as $\Delta\varepsilon = 4.62 \times 10^{-3}$ according to their resonant equation $n = mc/(2\pi Rf)$, where n is the mode index, m is the azimuthal mode number, R is the radius of the microsphere and f is the resonant frequency.

At the presence of g in the Faraday microcavity, the intrinsic polarizations of the WGMs become to the regular elliptical polarizations, i.e., right elliptical polarization (REP) with its major axis along the r direction and left elliptical polarization (LEP) with its major axis along the z direction. With the increase of g, the ellipticity angles of REP and LEP will increase, but the orientation angles remain unchanged. The similar results have been shown in the Poincaré sphere of Fig. 5 except the coupling range $(g1, g5)$, which will be discussed in detail below. At the same time, the resonant frequency of the LEP mode increases with g. On the contrary, the frequency of the REP mode decreases with g. When g is greater than 2.3×10^{-3}, Faraday effect is more dominant than linear birefringence in the cavity, so the resonant frequency of REP and LEP mode will change with g almost linearly [20], but with the opposite slope. The frequency of LEP mode increases, but REP decreases linearly. As a result, the dispersion curve of the REP mode intersects with that of the LEP mode at $g \approx 2.5 \times 10^{-3}$ with their mode numbers $\Delta m = \Delta l = \pm1$, at $g \approx 6.5 \times 10^{-3}$ with their mode numbers $\Delta m = \Delta l = \pm2$, and so on. Although two fundamental modes can intersect with each other, no mode coupling is observed due to phase mismatching ($\Delta m \neq 0$).

Then we study the properties of the mode coupling between the REP and LEP modes in a Faraday microcavity, including their resonant frequencies and mode polarizations. To satisfy the phase matching, the azimuthal mode number m of two modes is fixed at the same 586. The coupled modes are left elliptically-polarized fundamental mode (1, 586, 586, LEP) and right elliptically-polarized mode (1, 587, 586, REP). As shown in Fig. 3, the REP mode is coupled with the LEP mode to produce the anti-crossing couplings of the resonant frequencies and polarizations within the coupling range $(2.5100, 2.5126)(\times10^{-3})$. The strong coupling mixes the original intrinsic LEP/REP modes into the supermodes, which also brings the severe changes of their mode field distributions and polarizations in a narrow coupling range. In Fig. 3, the supermodes have two
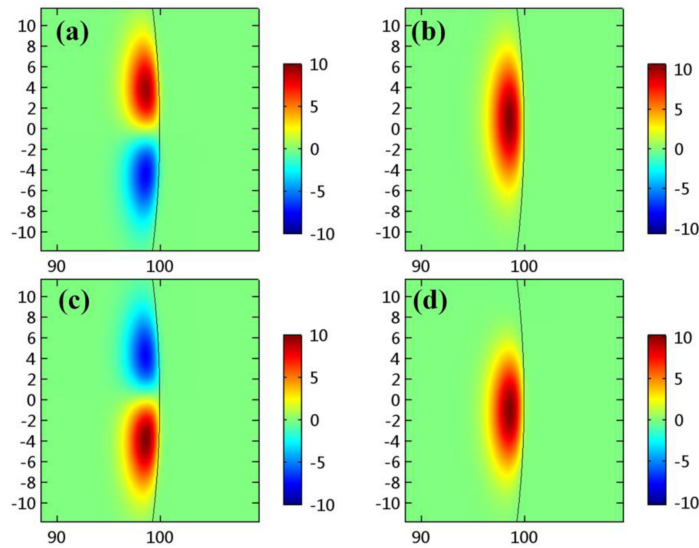
Fig. 4. Components on rz-plane for the supermodes at $g = 2.5113 \times 10^{-3}$. (a) and (b), H_r and H_z of 1st supermode; (c) and (d), H_r and H_z of 2nd supermode, respectively.

branches, and the lower and upper branch are named as 1st supermode and 2nd supermode, respectively. At $g = 2.5113 \times 10^{-3}$, the mode coupling is strongest, and the frequency difference of two supermodes is about 73.4MHz. According to the theory of mode coupling, the coupling coefficient in our system is estimated at about 36.7MHz [23]. If the Q factor of such this Faraday microcavity is reduced from 10^7 to 10^3, the coupling coefficient will be reduced about 1000 times, so the higher Q factor can enhance the MO interaction efficiently.

The field distributions of the supermodes at $g = 2.5113 \times 10^{-3}$ are shown in Fig. 4. The components H_r and H_z of the 1st supermode are shown in Figs. 4(a) and (b). It is obviously shown that the mode field of the supermode is the addition of mode (1, 586, 586, LEP) and (1, 587, 586, REP). At the strongest coupling point, the component H_r has almost the same amplitude and energy as H_z, and two components couple with each other most efficiently due to Faraday effect. Also, the components of the 2nd supermode are shown in Figs. 4(c) and (d). Its component H_z is similar to the 1st supermode, but H_r is the mirror of H_r component of 1st supermode. Thus they can build the different polarizations, as shown in Fig. 3.

For the resonant WGM in the microcavity, its polarization can be described by a polarization ellipse in rz-plane of cylindrical coordinates, as shown in Fig. 4. To visually describe the dynamic polarization evolutions of the supermodes with the gyration vector g, their polarizations are projected onto the Poincaré sphere, as shown in Fig. 5. In addition, the polarizations of the intrinsic modes out of mode coupling range are included. Each point on the Poincaré sphere represents a different polarization. And the ellipticity and orientation angles of the polarization ellipse correspond to the half polar and azimuthal angles of Poincaré sphere, respectively.

As shown in Fig. 5(a), we can clearly observe the polarization evolution of 1st/2nd supermode with g according to the blue/red trajectory on the Poincaré sphere. For 1st supermode, at $g0 = 0$, the polarization of WGM is a linear TM polarization along the z direction, shown in Fig 5(b). As g increases from $g0$ to $g1 = 2.3 \times 10^{-3}$, the polarization trajectory moves along the longitude line of the sphere towards the north pole, suggesting that the intrinsic polarization becomes the LEP with the fixed major axis direction (z direction), but the ellipticity angle of the polarization ellipse increases as the increase of g. Then, as g increases into the coupling range from $g1$ to $g5$, the polarization trajectory will move quickly from the north hemisphere to the south hemisphere due to the mode coupling. During this process, both the ellipticity and the orientation of polarization ellipse change severely due to mode coupling. Some of polarization ellipses at $g2$, $g3$ and $g4$ are shown in Fig. 5(b). Especially, the linear polarization with about the orientation angle of $\pi/4$ is generated
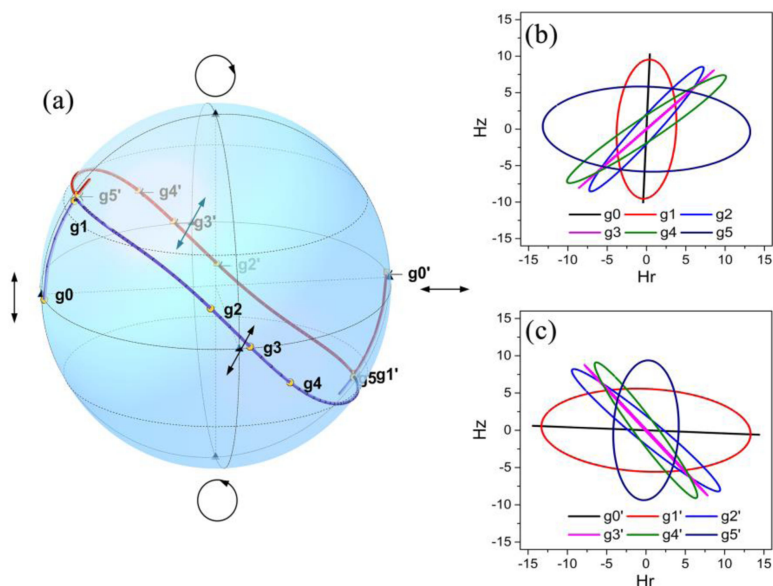
Fig. 5. (a) Polarization evolutions of 1st supermode (blue line) and 2nd supermode (red line) on Poincaré sphere. (b) The typical polarization ellipses of 1st supermode at $(g0, g1, g2, g3, g4, g5) = (0, 2.3000, 2.5105, 2.5109, 2.5113, 2.6000) \times 10^{-3}$, respectively. (c) The polarization ellipses of 2nd supermode at $(g0', g1', g2', g3', g4', g5') = (0, 2.4000, 2.5113, 2.5117, 2.5121, 2.7000) \times 10^{-3}$, respectively.

at around $g3$. And In the narrower range $(g2, g4)$ of strong coupling, the change of the orientation angle of the supermode is enhanced greatly more than 2 orders of magnitude, compared with that out of strong coupling range. Finally, as g increases greater than $g5$, the coupled mode gradually degenerates to the intrinsic mode (such as shown in Fig. 2), whose polarization is the REP with the fixed r direction of major axis. If g is large enough, the right circularly polarization can be achieved theoretically. Meanwhile, the polarization evolution of 2nd supermode is studied in Figs. 5(a) and (c), which is similar to 1st supermode. In the coupling range, the polarization changes greatly, and is enhanced greatly by the mode coupling. Out of the coupling range, the mode shows the normally intrinsic LEP or REP.

4. Conclusion

In summary, we have studied the polarization coupling in a high Q Faraday microsphere. In the Faraday microcavity, the intrinsic polarization of WGM is the left or right elliptical polarization. These two polarizations have the opposite dispersion curves. As the gyration vector g increases, the resonant frequency of LEP increases, while the resonant frequency of REP decreases. So these two polarization modes with the same azimuthal mode number m can couple with each other due to the Faraday effect, and strong polarization coupling is achieved. We have studied the mode characteristics of polarization coupling, such as the polarization evolution and mode distribution. Through polarization coupling, the elliptical polarization with different ellipticity and orientation angles can be generated. Such the mode coupling may possess the applications related to polarization modulation.

References

[1] K. J. Vahala, "Optical microcavities," *Nature*, vol. 424, no. 6950, pp. 839–846, 2003.
[2] T. J. Kippenberg, S. M. Spillane, D. K. Armani, and K. J. Vahala, "Ultralow-threshold microcavity Raman laser on a microelectronic chip," *Opt. Lett.*, vol. 29, no. 11, pp. 1224–1226, 2004.

[3] S. M. Spillane, T. J. Kippenberg, and K. J. Vahala, "Ultralow-threshold Raman laser using a spherical dielectric microcavity," *Nature*, vol. 415, no. 6872, pp. 621–623, 2002.

[4] S. Arnold, S. I. Shopova, and S. Holler, "Whispering gallery mode bio-sensor for label-free detection of single molecules: thermo-optic vs. reactive mechanism," *Opt. Express*, vol. 18, no. 1, pp. 281–287, 2010.

[5] J. M. Ward and O. Benson, "WGM microresonators: sensing, lasing and fundamental optics with microspheres," *Laser Photon. Rev.*, vol. 5, no. 4, pp. 553–570, 2011.

[6] P. Delhaye, T. Herr, E. Gavartin, M. L. Gorodetsky, R. Holzwarth, and T. J. Kippenberg, "Octave spanning tunable frequency comb from a microresonator," *Phys. Rev. Lett.*, vol. 107, no. 6, 2011, Art. no. 063901.

[7] T. J. Kippenberg, R. Holzwarth, and S. A. Diddams, "Microresonator-based optical frequency combs," *Science*, vol. 332, no. 6029, pp. 555–559, 2011.

[8] M. J. Freiser, "A survey of magnetooptic effects," *IEEE Trans. Magn.*, vol. 4, no. 2, pp. 152–161, Jun. 1968.

[9] M. N. Deeter, "Fiber-optic faraday-effect magnetic-field sensor based on flux concentrators," *Appl. Opt.*, vol. 35, no. 1, pp. 154–157, 1996.

[10] H. Dotsch *et al.*, "Applications of magneto-optical waveguides in integrated optics," *J. Opt. Soc. Amer. B*, vol. 22, no. 1, pp. 240–253, 2005.

[11] L. Bi *et al.*, "On-chip optical isolation in monolithically integrated non-reciprocal optical resonators," *Nat. Photon.*, vol. 5, no. 12, pp. 758–762, 2011.

[12] H. Huebl *et al.*, "High cooperativity in coupled microwave resonator ferrimagnetic insulator hybrids," *Phys. Rev. Lett.*, vol. 111, no. 12, 2013, Art. no. 127003.

[13] X. Zhang, C. L. Zou, L. Jiang, and H. X. Tang, "Strongly coupled magnons and cavity microwave photons," *Phys. Rev. Lett.*, vol. 113, no. 15, 2014, Art. no. 156401.

[14] X. Zhang, N. Zhu, C. Zou, and H. X. Tang, "Optomagnonic whispering gallery microresonators," *Phys. Rev. Lett.*, vol. 117, no. 12, pp. 123605–123605, 2016.

[15] J. A. Haigh, A. Nunnenkamp, A. J. Ramsay, and A. J. Ferguson, "Triple-resonant Brillouin light scattering in magneto-optical cavities," *Phys. Rev. Lett.*, vol. 117, no. 13, 2016, Art. no. 133602.

[16] J. A. Haigh *et al.*, "Magneto-optical coupling in whispering-gallery-mode resonators," *Phys. Rev A*, vol. 92, no. 6, 2015, Art. no. 063845.

[17] A. Osada *et al.*, "Cavity optomagnonics with spin-orbit coupled photons," *Phys. Rev. Lett.*, vol. 116, no. 22, 2016, Art. no. 223601.

[18] C. Z. Chai, H. Q. Zhao, H. X. Tang, G. C. Guo, C. L. Zou, and C. H. Dong, "Non-reciprocity in high-Q ferromagnetic microspheres via photonic spin–orbit coupling," *Laser Photon. Rev.*, vol. 14, no. 2, 2019, Art. no. 1900252.

[19] P. S. Pershan, "Magneto-optical Effects," *J. Appl. Phys.*, vol. 38, no. 3, pp. 1482–1490, 1967.

[20] A. K. Zvezdin and V. A. Kotov, *Modern Magnetooptics and Magnetooptical Mterials*. Boca Raton, FL, USA: CRC Press, 1997.

[21] I. H. Malitson, "Interspecimen comparison of the refractive index of fused silica," *J. Opt. Soc. Amer.*, vol. 55, no. 10, pp. 1205–1209, 1965.

[22] M. Oxborrow, "Traceable 2-D finite-element simulation of the whispering-gallery modes of axisymmetric electromagnetic resonators," *IEEE Trans Microw. Theory Tech.*, vol. 55, no. 6, pp. 1209–1218, Jun. 2007.

[23] H. A. Haus, *Waves and Fields in Optoelectronics*. Englewood Cliffs, NJ, USA: Prentice-Hall, 1984.